Electronic Supplementary Material (ESI) for Dalton Transactions.
This journal is © The Royal Society of Chemistry 2018

Electronic Supplementary Material (ESI) for Dalton Transactions.

This journal is © The Royal Society of Chemistry 2018

Two Photochromic Iodoargentate Hybrids with Adjustable Photoresponsive Mechanism

Electronic Supplementary Information

Xia Li, Pengfei Hao,* Junju Shen and Yunlong Fu*

Key Laboratory of Magnetic Molecules, Magnetic Information Materials Ministry of Education, School of Chemical and Material Science, Shanxi Normal University, Linfen 041004, China

Content

1. Chemical analysis for photolytic products

Dissolve compounds **1** (0.534 g, 0.5 mmol), **1P** (0.534 g, 0.5 mmol), **2** (0.255 g, 0.5 mmol), **2P** (0.255 g, 0.5 mmol) in 5 mL dimethyl sulfoxide containing 0.15 g NaI respectively. The resultant solution are colorless for **1** and **2**, while the solution for **1P** and **2P** are yellowish and decolored after addition of excess $Na_2S_2O_3$ (0.158 g, 1 mmol), implying existence of I_3^-. Several minutes later, the black precipitated particles are observed in the solution of **1P** and **2P**, and further verified as metal silver through a classical procedure. The whole process is carried out in the dark at room temperature.

2. Figures

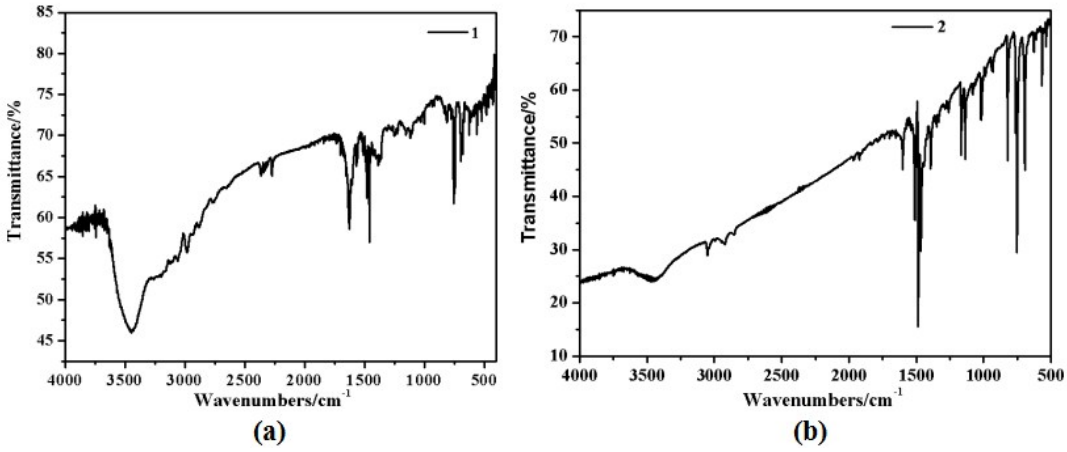

Fig. S1 IR spectra of **1** and **2**.

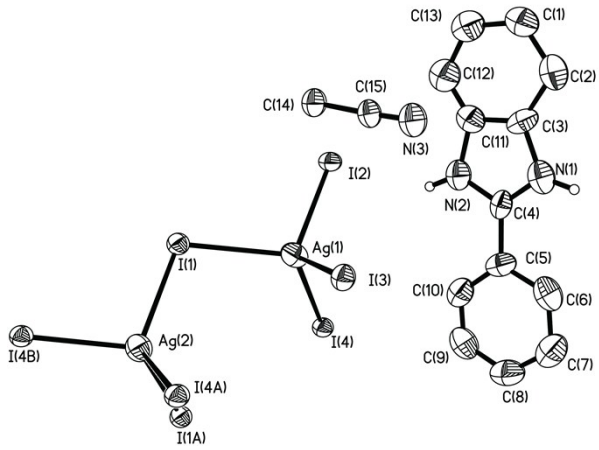

Fig. S2 The asymmetric unit of **1**.

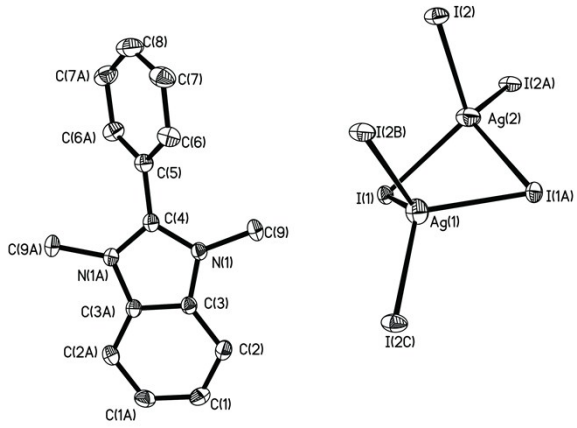

Fig. S3 The asymmetric unit of **2**.

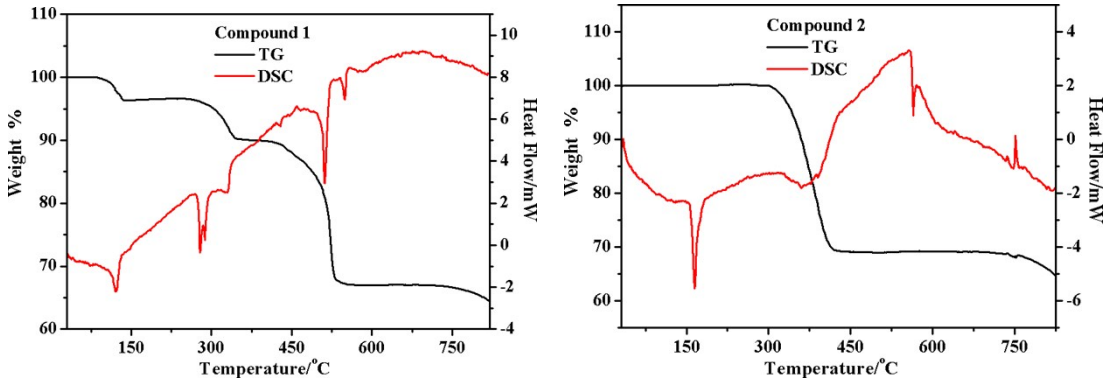

Fig. S4 Thermo-gravimetric (TG) and differential scanning calorimetry (DSC) curves of **1** (left) and **2** (right).

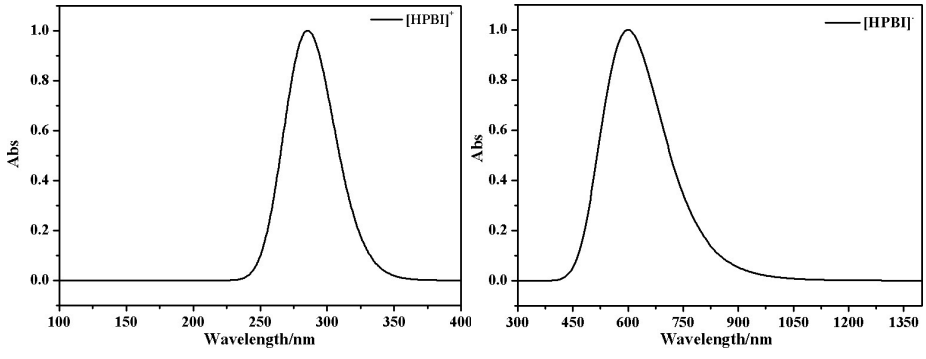

Fig. S5 The calculated UV-vis spectra of $[HPBI]^+$ cation (left) and $[HPBI]^\bullet$ radicals (right) through density functional theory (DFT) computations using the Gaussian 09 suite of programs[S1]. A hybrid functional B3LYP was used for all calculations.

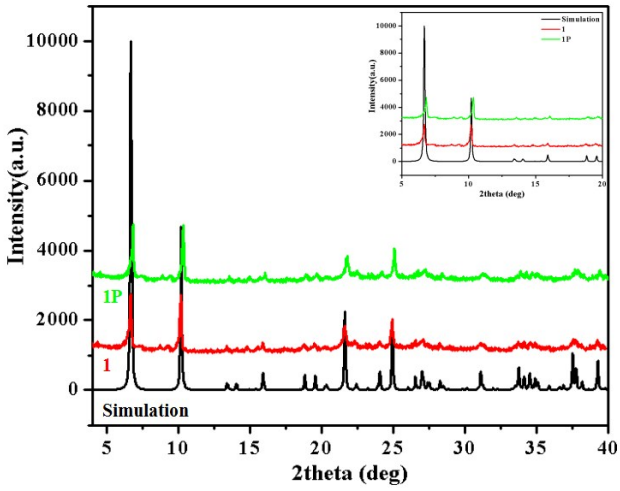

Fig. S6 Powder X-ray diffraction (PXRD) of **1** (before irradiation) and **1P** (after irradiation) at room temperature (RT). The inset shows some diffraction peaks of **1P** slightly shift to high angles compared with **1**.

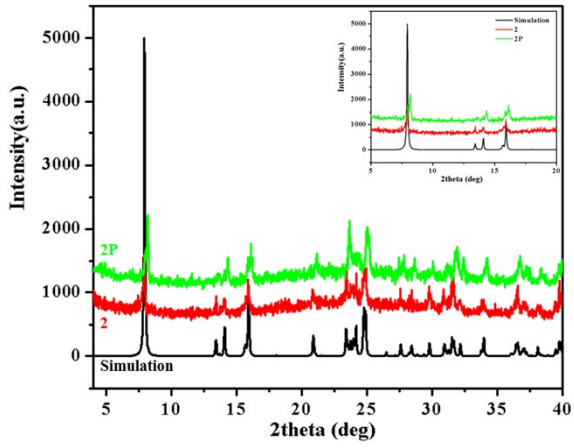

Fig. S7 Powder X-ray diffraction (PXRD) of **2** (before irradiation) and **2P** (after irradiation) at room temperature (RT). The inset shows some diffraction peaks of **2P** slightly shift to high angles compared with **2**.

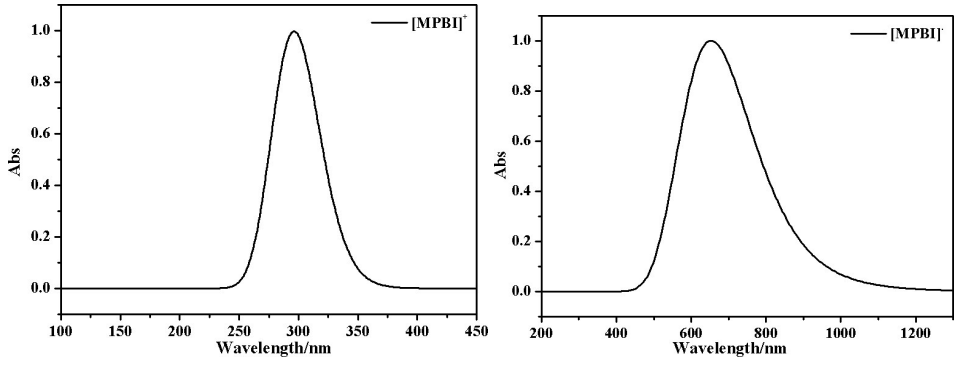

Fig. S8 The calculated UV-vis spectra of $[MPBI]^+$ cations (left) and $[MPBI]^\bullet$ radicals (right) through density functional theory (DFT) computations using the Gaussian 09 suite of programs[S1]. A hybrid functional B3LYP was used for all calculations.

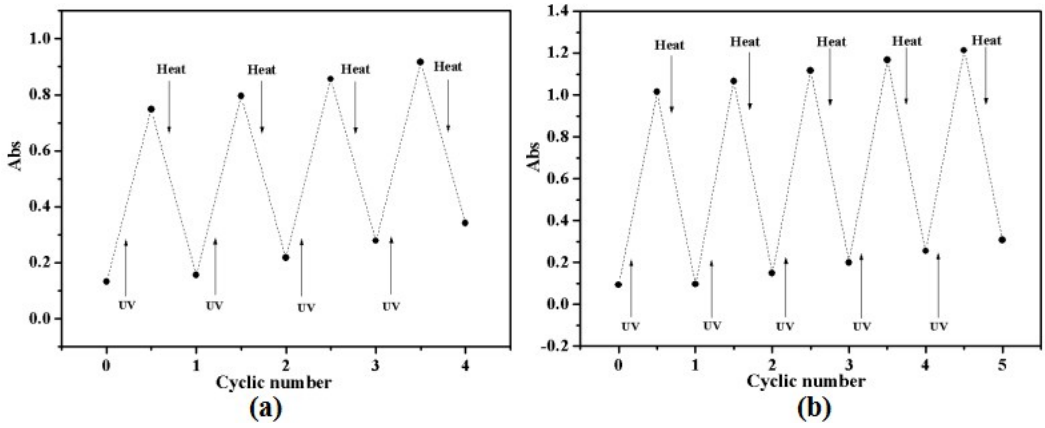

Fig. S9 The absorption changes with repeated ultraviolet irradiation/heat cycles of **1** (a) at 430 nm and **2** (b) at 450 nm.

3. Tables

Table S1 Crystal data and structure refinement for **1** and **2**.

Compound	**1**	**2**
CCDC code	1820806	1820807
Empirical formula	$C_{15}H_{14}N_3Ag_3I_4$	$C_{15}H_{15}N_2Ag_3I_4$
Temperature	273(2) K	273(2) K
Formula weight	1067.50	1054.50
Crystal size	0.424 x 0.058 x 0.047	0.032×0.13×0.423
Crystal system	Monoclinic	Orthorhombic
Space group	*C2/m*	*Pnna*
a (Å)	26.757(7)	7.5462(4)
b (Å)	6.7094(17)	22.2417(12)
c (Å)	13.283(3)	13.1833(7)
α (°)	90	90
β (°)	98.927(6)	90
γ (°)	90	90
V (Å^3)	2355.8(10)	2212.7(2)
Z	4	4
D_c (g/cm^3)	3.010	3.165
F (000)	1912.0	1888.0
μ (mm^{-1})	7.716	8.211
Reflections collected	36335	37421
Unique reflections	3129	2715
R_{int}	0.0240	0.0305
F^2	1.084	1.093
$R_1/wR_2[I\geq2\sigma(I)]$	0.0488, 0.1377	0.0364, 0.0929
R_1/wR_2 (all date)	0.0582, 0.1512	0.0386, 0.0944
$\Delta\rho_{max}/\Delta\rho_{min}$ (e Å^{-3})	1.818, -1.822	1.499, -1.923

$^aR_1 = \sum||F_o|-|F_c||/\sum|F_o|$, $^bwR_2 = [\sum w(F_o^2-F_c^2)^2/\sum w(F_o^2)^2]^{1/2}$

Table S2 Selected bond lengths (Å) and angles (°) for **1** and **2**.

Compound **1**			
Ag(1)-I(3)	2.7801(6)	Ag(1)-I(2)	2.8076(6)
Ag(1)-I(4)	2.9610(6)	Ag(1)-I(1)	2.9656(7)
Ag(2)-I(4)#2	2.8709(6)	Ag(2)-I(4)#3	2.8709(6)
Ag(2)-I(1)#2	2.8756(6)	Ag(2)-I(1)	2.8756(6)
Ag(1)-Ag(1)#1	3.1512(10)	Ag(1)-Ag(2)#2	3.2034(7)
Ag(2)-Ag(1)#1	3.2034(7)	Ag(2)-Ag(1)#2	3.2034(7)
Ag(2)-Ag(2)#4	3.2747(12)		
I(3)-Ag(1)-I(2)	110.064(17)	I(3)-Ag(1)-I(4)	113.236(16)
I(2)-Ag(1)-I(4)	103.69(2)	I(3)-Ag(1)-I(1)	113.00(2)
I(2)-Ag(1)-I(1)	105.420(16)	I(4)-Ag(1)-I(1)	110.729(15)
I(4)#2-Ag(2)-I(4)#3	110.45(2)	I(4)#2-Ag(2)-I(1)#2	116.112(12)
I(4)#3-Ag(2)-I(1)#2	103.950(13)	I(4)#2-Ag(2)-I(1)	103.950(13)
I(4)#3-Ag(2)-I(1)	116.112(12)	I(1)#2-Ag(2)-I(1)	106.66(2)
Symmetry code: #1 x,-y+2,z #2 -x+2,-y+2,-z #3 x,y+1,z #4 -x+2,-y+3,-z #5 x,-y+1,z #6 x,y-1,z			
Compound **2**			
Ag(2)-I(2)#1	2.8204(7)	Ag(2)-I(2)	2.8233(7)
Ag(2)-I(1)#2	2.8853(6)	Ag(2)-I(1)	2.9128(6)
Ag(1)-I(2)#3	2.8239(5)	Ag(1)-I(2)#4	2.8239(6)
Ag(1)-I(1)	2.8879(6)	Ag(1)-I(1)#2	2.8879(6)
I(2)#1-Ag(2)-I(2)	101.312(17)	I(2)#1-Ag(2)-I(1)#2	118.08(2)
I(2)-Ag(2)-I(1)#2	116.86(2)	I(2)#1-Ag(2)-I(1)	113.85(2)
I(2)-Ag(2)-I(1)	116.02(2)	I(1)#2-Ag(2)-I(1)	91.650(18)
I(2)#3-Ag(1)-I(2)#4	102.92(3)	I(2)#3-Ag(1)-I(1)	113.957(11)
I(2)#4-Ag(1)-I(1)	117.304(10)	I(2)#3-Ag(1)-I(1)#2	117.304(10)
I(2)#4-Ag(1)-I(1)#2	113.957(11)	I(1)-Ag(1)-I(1)#2	92.11(2)
Symmetry code: #1 x-1/2,y,-z+2 #2 x,-y+3/2,-z+3/2 #3 x+1/2,y,-z+2 #4 x+1/2,-y+3/2,z-1/2 #5 -x+3/2,-y+1,z			

Table S3 Theoretical lowest unoccupied molecular orbital (LUMO) energy of specific organic cations and photochromic mechanism of their iodoargentates.

Organic cations	LUMO (eV)[a]	Photochromic mechanism
N,*N* -dimethyl-2-phenylbenzimidazolium	-5.1713	Photolysis + Photoinduced ET
N-proton-2-phenylbenzimidazolium	-5.7419	Photolysis
Monoprotonated pyrazinium	-8.0968	Photoinduced ET
N-methyl-4-carbomethoxypyridinium	-9.7126	Photoinduced ET
N-methyl-nicotinohydrazide	-10.1181	Photoinduced ET

[a] The theoretical values of organic cations through density functional theory (DFT) computations using the Gaussian 09 suite of programs[S1]. A hybrid functional, B3LYP, was used for all calculations. Geometry was optimized using the 6-31G basis set.

Reference

S1 M. J. Frisch, G. W. Trucks, H. B. Schlegel, G. E. Scuseria, M. A. Robb, J. R. Cheeseman, G. Scalmani, V. Barone, B. Mennucci, G. A. Petersson, H. Nakatsuji, M. Caricato, X. Li, H. P. Hratchian, A. F. Izmaylov, J. Bloino, G. Zheng, J. L. Sonnenberg, M. Hada, M. Ehara, K. Toyota, R. Fukuda, J. Hasegawa, M. Ishida, T. Nakajima, Y. Honda, O. Kitao, H. Nakai, T. Vreven , J. A. Montgomery, J. E. Peralta, F. Ogliaro, M. Bearpark, J. J. Heyd, E. Brothers, K. N. Kudin, V. N. Staroverov, T. Keith, R. Kobayashi, J. Normand, K. Raghavachari, A. Rendell, J. C. Burant, S. S. Iyengar, J. Tomasi, M. Cossi, N. Rega, J. M. Millam, M. Klene, J. E. Knox, J. B. Cross, V. Bakken, C. Adamo, J. Jaramillo , R. Gomperts , R. E. Stratmann, O. Yazyev, A. J. Austin, R. Cammi, C. Pomelli, J. W. Ochterski , R. L. Martin, K. Morokuma, V. G. Zakrzewski, G. A. Voth, P. Salvador, J. J. Dannenberg, S. Dapprich, A. D. Daniels, O. Farkas, J. B. Foresman, J. V. Ortiz, J. Cioslowski and D. J. Fox, Gaussian 09, Revision D. 01, Gaussian Inc., Wallingford, CT, 2013